LOCKHEED MARTIN ENERGY RESEARCH LIBRARIES
3 4456 0515555 0

CENTRAL RESEARCH LIBRARY
DOCUMENT COLLECTION

ORNL-4364
UC-4 – Chemistry

Cy 2

UNIT OPERATIONS SECTION

QUARTERLY PROGRESS REPORT

JANUARY–MARCH 1968

OAK RIDGE NATIONAL LABORATORY
CENTRAL RESEARCH LIBRARY
DOCUMENT COLLECTION
LIBRARY LOAN COPY
DO NOT TRANSFER TO ANOTHER PERSON
If you wish someone else to see this document, send in name with document and the library will arrange a loan.
UCN-7969
(3 3-67)

OAK RIDGE NATIONAL LABORATORY
operated by
UNION CARBIDE CORPORATION
for the
U.S. ATOMIC ENERGY COMMISSION

Printed in the United States of America. Available from Clearinghouse for Federal Scientific and Technical Information, National Bureau of Standards, U.S. Department of Commerce, Springfield, Virginia 22151
Price: Printed Copy $3.00; Microfiche $0.65

LEGAL NOTICE

This report was prepared as an account of Government sponsored work. Neither the United States, nor the Commission, nor any person acting on behalf of the Commission:

A. Makes any warranty or representation, expressed or implied, with respect to the accuracy, completeness, or usefulness of the information contained in this report, or that the use of any information, apparatus, method, or process disclosed in this report may not infringe privately owned rights; or

B. Assumes any liabilities with respect to the use of, or for damages resulting from the use of any information, apparatus, method, or process disclosed in this report.

As used in the above, "person acting on behalf of the Commission" includes any employee or contractor of the Commission, or employee of such contractor, to the extent that such employee or contractor of the Commission, or employee of such contractor prepares, disseminates, or provides access to, any information pursuant to his employment or contract with the Commission, or his employment with such contractor.

ORNL-4364

Contract No. W-7405-eng-26

UNIT OPERATIONS SECTION QUARTERLY PROGRESS REPORT

January-March 1968

CHEMICAL TECHNOLOGY DIVISION

M. E. Whatley

P. A. Haas
L. E. McNeese
A. D. Ryon
C. D. Watson

OCTOBER 1969

OAK RIDGE NATIONAL LABORATORY
Oak Ridge, Tennessee
Operated by
UNION CARBIDE CORPORATION
for the
U. S. ATOMIC ENERGY COMMISSION

LOCKHEED MARTIN ENERGY RESEARCH LIBRARIES

3 4456 0515555 0

CONTENTS

Page

ABSTRACTS 1

1. CHEMICAL ENGINEERING RESEARCH 3

1.1 Stacked-Clone Contactor. 3

2. MOLTEN-SALT REACTOR PROCESSING STUDIES 12

2.1 MSRE Distillation Experiment 13

2.1.1 Operating Procedures 13

2.1.2 Experimental Results 15

2.1.3 Operational Difficulties 17

2.1.3.1 Conductivity-Type Level Indicators 18

2.1.3.2 Sampling Difficulties 18

2.1.3.3 Feed Line Deposit 19

2.1.4 Conclusions 19

2.2 Removal of Protactinium from a Single-Fluid MSBR 20

2.3 Continuous Fluorination of Molten Salt 28

2.4 Removal of Nickel, Iron, and Chromium Fluorides from Simulated MSRE Fuel Carrier Salt 31

2.4.1 Reduction of Corrosion-Product Fluorides 32

2.4.2 Salt Filtration Studies 37

ABSTRACTS

1. CHEMICAL ENGINEERING RESEARCH

By virtue of its very short solvent-residence time per stage, the stacked-clone solvent-extraction contactor is especially suitable for use in reprocessing schemes involving highly radioactive, short-cooled fuels, for example, from fast breeder reactors (FBR). Therefore, tests were made to evaluate flow capacities and mass-transfer efficiencies of the prototype stacked-clone contactor in a system that simulated conditions of an FBR fuel reprocessing flowsheet. Uranium processing rates as high as 41 kg/day were realized at stage efficiencies of about 50%.

2. MOLTEN-SALT REACTOR PROCESSING STUDIES

A molten-salt breeder reactor (MSBR) will be fueled with a molten fluoride mixture that will circulate continuously through the reactor core and the primary heat exchanger. A close-coupled processing facility for removing fission products and fissile materials from this mixture will be an integral part of the reactor system.

Low-pressure distillation is one method being considered for separating the rare-earth fission products (i.e. fission products having fluorides of low volatility) from the more-volatile components of the fuel salt. Experimentally determined relative volatilities indicate that adequate removal of the rare-earth fluorides from fuel salt can be accomplished. Results of distillation experiments with nonradioactive salt having the composition of the MSRE fuel carrier salt, $LiF-BeF_2-ZrF_4$ (65-30-5 mole %), are presented.

In order to obtain a high breeding ratio in an MSBR, a low protactinium concentration must be maintained in regions of high neutron flux. This avoids parasitic capture in the protactinium before it decays to uranium. Presently, the main emphasis is on processing a single-fluid MSBR in which protactinium must be separated from uranium, thorium, and fission products.

A flowsheet that uses reductive extraction for isolating protactinium from a single-fluid MSBR has been proposed, and results of the performance of the isolation system under steady-state conditions have been calculated. These calculations were based on laboratory data on the distribution of materials of interest between molten salt and liquid bismuth containing a reductant.

The continuous fluorination of a molten salt is being studied as a means of removing uranium. Equipment is being developed for the continuous removal of UF_4 from a salt stream by countercurrently contacting the salt with fluorine in a salt-phase-continuous system. The equipment will be protected from corrosion by freezing a layer of salt on the vessel wall; the heat necessary for maintaining molten salt adjacent to the frozen salt layer will be provided by the decay of fission products in the salt stream. Initial experiments designed to demonstrate the operability of a frozen-wall fluorinator, using a countercurrent flow of molten salt and an inert gas, were completed.

Current plans for the MSRE include the substitution of ^{233}U for the mixture of ^{235}U and ^{238}U presently in the fuel salt. The fuel carrier salt, together with its fission-product inventory, will be retained; this will require fluorination of the fuel salt, to remove the uranium, and the subsequent addition of ^{233}U. During fluorination, the salt will become contaminated with the fluorides of nickel, iron, and chromium as a result of the corrosion of the fluorinator, which is constructed of Hastelloy N. The return of these fluorides to the reactor is undesirable. Experiments were carried out in which the corrosion-product fluorides were reduced, using hydrogen and zirconium metal, and the reduced metals were separated from the simulated fuel carrier salt by decantation and filtration.

<u>Previous Reports in This Series for the Year 1967</u>

January-March	ORNL-4139
April-June	ORNL-4204
July-September	ORNL-4234
October-December	ORNL-4235

1. CHEMICAL ENGINEERING RESEARCH

1.1 Stacked-Clone Contactor

W. S. Groenier

In its present state of development, the stacked-clone contactor is a device that is capable of performing stagewise countercurrent solvent extractions at a high flow capacity, a very short residence time per stage, and high stage efficiencies. These attributes promise successful application to reprocessing schemes involving highly radioactive, short-cooled fuels, for example, from fast breeder reactors (FBR).

During this report period the 18-stage prototype stainless steel stacked-clone contactor was tested, using a system that simulated conditions of a first-cycle FBR reprocessing flowsheet. However, feed solutions did not contain particulate matter, and no attempt was made to simulate the presence of fission products. The chemical system was composed of an aqueous feed that was about 3 M in HNO_3 and contained ~ 70 g of uranium and ~3 g of thorium per liter, an aqueous scrub solution that was about 2 M in HNO_3, and an organic feed that contained about 15 vol % tributyl phosphate (TBP) in an aliphatic hydrocarbon diluent (similar to n-dodecane). The thorium was included to allow scrubbing efficiencies to be measured. Of a total of 15 runs, eight were made with the aqueous phase continuous, and seven were made with the organic phase continuous. Scrubbing was omitted in the control runs made in each mode. Nominal flow ratios (aqueous:organic) were 0.65 in the extraction zone and 0.15 in the scrub zone. The results are tabluated in Tables 1.1 and 1.2; physical properties are listed in Table 1.3. Figures 1.1 and 1.2 represent McCabe-Thiele diagrams for uranium and thorium, respectively, for a typical run; theoretical extraction and scrubbing stages are shown. The distribution coefficients of uranium and thorium in the chemical system described above are related as shown in Fig. 1.3.

Table 1.1 **Performance Data for Prototype Stacked-Clone Contactor Operation with a Simulated FBR Flowsheet: Aqueous-Continuous Mode**

Temperature: 40°C

Run Designation	AC-1	AC-2	AC-3	AC-4	AC-5	AC-6	AC-7	AC-8
Aqueous Feed: Uranium (g/liter)	66.9	66.9	66.9	73.8	73.8	73.8	55.7	55.7
Thorium (g/liter)	3.36	3.36	3.36	2.89	2.89	2.89	2.26	2.26
Acid Concentration (M)	2.79	2.79	2.79	2.94	2.94	2.94	2.75	2.75
Scrub Feed: Acid Concentration (M)	1.85	1.85	1.85	1.95	1.95	1.95	---	---
Organic Feed: TBP (vol %)	13.4	13.6	13.5	15.8	15.8	15.8	16.15	16.15
Uranium (g/liter)	0.162	0.115	0.086	0.079	0.084	0.075	0.023	0.044
Organic Product: Uranium (g/liter)	35.0	36.1	36.2	33.2	36.5	35.2	33.05	40.45
Thorium (g/liter)	0.080	0.107	0.045	0.129	0.104	0.089	0.457	0.176
Acid Concentration (M)	0.115	0.111	0.094	0.155	0.152	0.140	0.184	0.153
Aqueous Raffinate: Uranium (g/liter)	0.335	0.117	0.419	0.111	0.209	0.219	0.0115	0.0610
Thorium (g/liter)	2.26	2.37	2.42	1.89	2.05	2.00	1.295	2.095
Acid Concentration (M)	2.41	2.44	2.45	2.46	2.51	2.49	2.39	2.54
Flow Ratio (A/O) in: Scrub Section	0.18	0.15	0.18	0.15	0.16	0.15	---	---
Extraction Section	0.71	0.68	0.75	0.61	0.64	0.64	0.59	0.74
Throughput of Run (liters/min)	0.79	0.97	1.31	1.19	1.06	1.28	1.12	1.22
Percent of Flooding	49	60	82	74	66	79	70	76
Uranium Material Balance (%)	100.3	102.3	96.0	98.5	102.1	98.2	100.2	98.7
Thorium Material Balance (%)	95.6	96.8	97.2	96.9	101.5	97.3	91.4	103.3
Uranium Loss to Raffinate (%)	0.7	0.2	0.8	0.2	0.4	0.4	0.02	0.1
Uranium Processing Rate (kg/day)	23.4	29.2	41.1	35.8	33.2	40.3	33.5	41.5
Decontamination Factor (Th from U)	22	17	40	10	14	16	3	9
No. of Physical Stages in: Scrub Section	5	5	5	8	8	8	---	---
Extraction Section	8	8	8	5	5	5	13	13
No. of Theoretical Stages in: Scrub Section	0.3	0.2	0.5	1.5	1.0	1.3	---	---
Extraction Section	3.4	3.9	3.5	3.2	3.1	3.0	4.2	4.0

Table 1.2 **Performance Data for Prototype Stacked-Clone Contactor Operation with a Simulated FBR Flowsheet: Organic-Continuous Mode**

Temperature 40°C

Run Designation	OC-1	OC-2	OC-3	OC-4	OC-5	OC-6	OC-7
Aqueous Feed: Uranium (g/liter)	68.4	70.0	70.2	66.2	67.6	55.6	55.6
Thorium (g/liter)	3.23	3.23	3.14	3.17	3.14	2.30	2.30
Acid Concentration (M)	2.89	2.89	2.89	2.89	2.89	2.73	2.73
Scrub Feed: Acid Concentration (M)	1.52	1.52	1.52	1.84	1.83		
Organic Feed: TBP (vol %)	14.01	14.02	14.03	14.16	14.14	15.93	15.93
Uranium (g/liter)	0.009	0.199	0.239	0.157	0.158	0.095	0.116
Organic Product: Uranium (g/liter)	31.2	32.3	29.6	29.7	27.0	37.5	36.1
Thorium (g/liter)	< 0.010	< 0.010	< 0.010	0.025	0.056	0.360	0.461
Acid Concentration (M)	0.099	0.100	0.101	0.104	0.108	0.159	0.167
Aqueous Raffinate: Uranium (g/liter)	1.27	2.23	0.755	0.430	0.207	0.073	0.043
Thorium (g/liter)	2.52	2.45	2.35	2.31	2.24	1.86	1.545
Acid Concentration (M)	2.45	2.41	2.37	2.37	2.37	2.54	2.515
Flow Ratio (A/O) in: Scrub Section	0.17	0.20	0.17	0.19	0.18	---	---
Extraction Section	0.76	0.80	0.60	0.63	0.59	0.67	0.66
Throughput of Run (liters/min)	0.89	0.90	0.89	0.72	0.76	0.71	0.78
Percent of Flooding	89	90	89	72	76	71	78
Uranium Material Balance (%)	78.8	80.8	99.8	103.0	98.3	100.1	98.4
Thorium Material Balance (%)	100.0	101.5	106.0	106.2	108.1	104.0	97.6
Uranium Loss to Raffinate (%)	2.4	4.3	1.5	0.9	0.5	0.1	0.08
Uranium Processing Rate (kg/day)	29.8	30.2	24.1	18.5	18.9	23.0	24.8
Decontamination Factor (Th from U)	>185	>185	>165	57	22	4	3
No. of Physical Stages in: Scrub Section	6	6	6	3	3	---	---
Extraction Section	5	5	5	8	8	11	11
No. of Theoretical Stages in: Scrub Section	2.5	2.3	3.0	1.8	1.7	---	---
Extraction Section	2.4	2.3	2.6	2.9	3.0	3.7	3.9

Table 1.3 Physical Properties of the Solutions

Solution	Temperature (°C)	Density (g/ml)	Viscosity (centipoises)	Interfacial Tension (dynes/cm)	Phase Ratio (A/O)	Batch Dispersion Break Time (sec) Organic Phase Continuous	Batch Dispersion Break Time (sec) Aqueous Phase Continuous
A[a]	25	1.112	0.95	17.9	0.10	33.6	----
					0.25	30.9	----
C[a]	25	0.817	1.58		0.65	42.6	----
					1	37.6	38.4
					4	----	27.0
					10	----	23.3
B[a]	25	1.068	0.89	13.8	0.10	37.5	----
					0.25	29.9	----
D[a]	25	0.741	1.31		0.65	33.5	26.1
					1	32.3	26.4
					4	----	24.1
					10	----	21.8

[a]Descriptions of the solutions are as follows: A — one volume of aqueous feed (69 g of uranium per liter, 3.2 g of thorium per liter, 2.8 M in H^+) plus 0.3 volume of scrub (1.85 M in H^+); B — aqueous raffinate (1 g of uranium per liter, 2.8 g of thorium per liter, 2.8 M in H^+); C — organic product (14.2 vol % TBP in n-paraffin diluent, equilibrated with solution A at a phase ratio of 1.3 parts of solution A to 2 parts of solution C); D — organic feed (14.2 vol % TBP in n-paraffin, no uranium).

ORNL DWG 69-4924

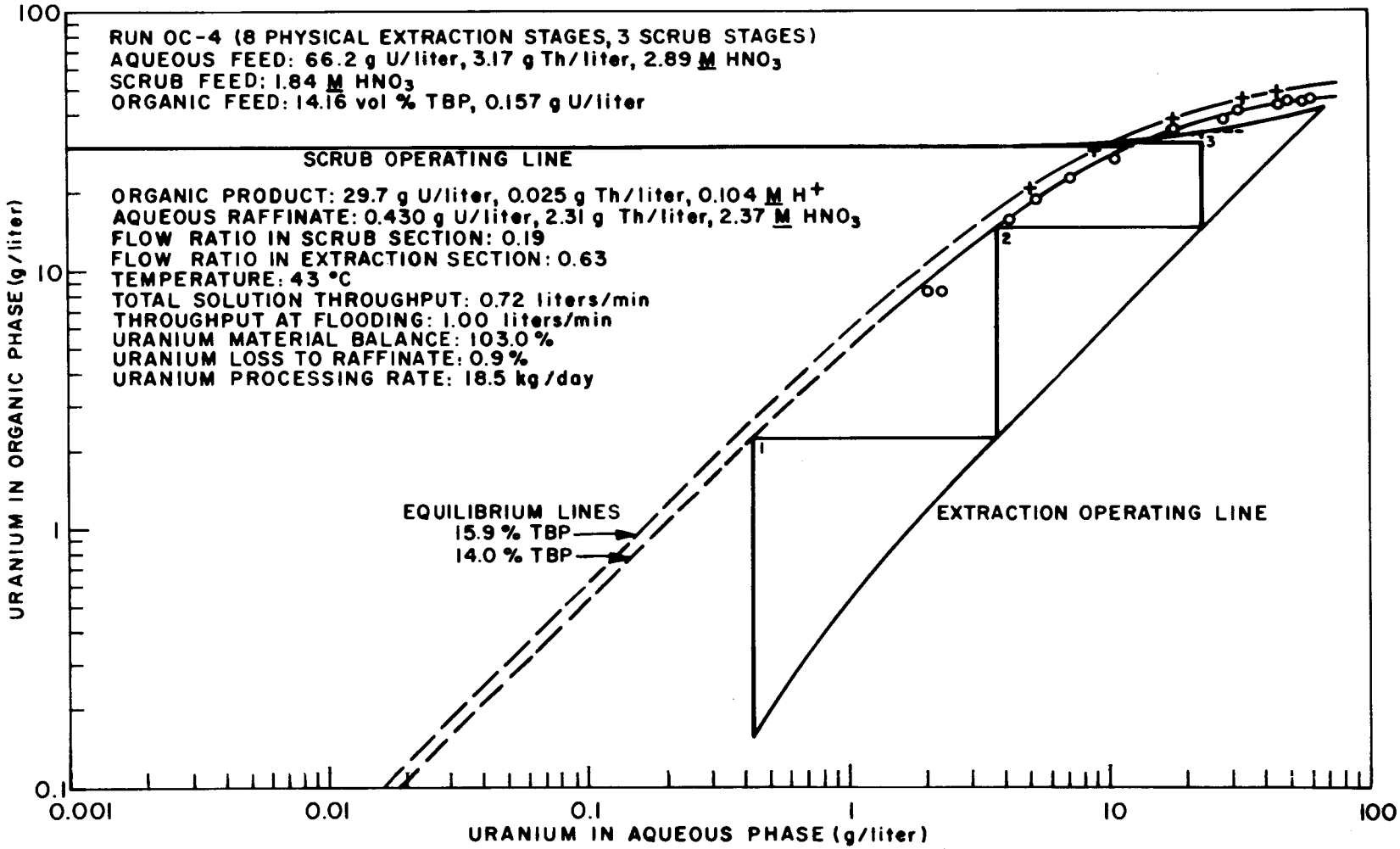

Fig. 1.1 McCabe-Thiele Diagram for Uranium.

ORNL DWG 69-4920

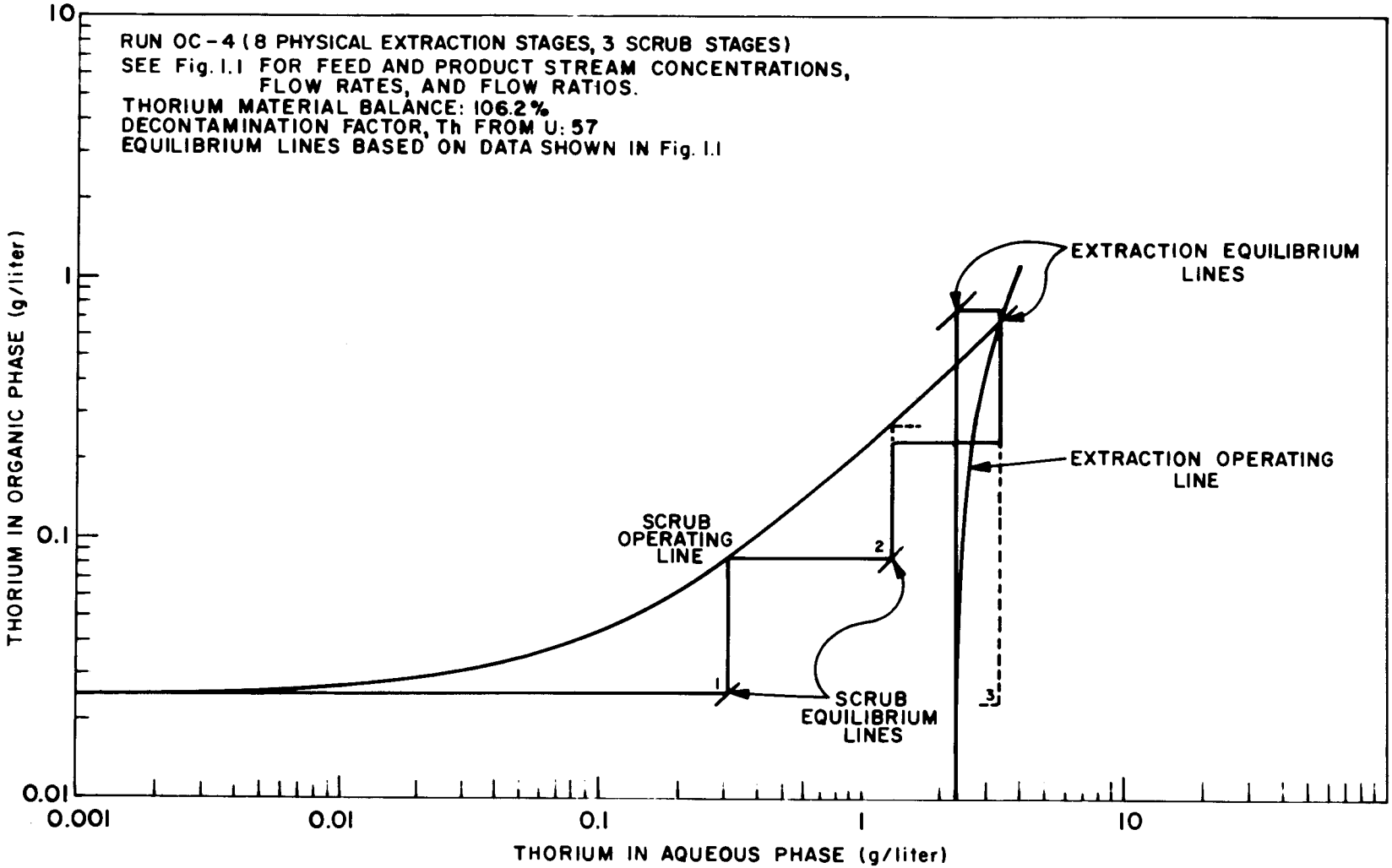

Fig. 1.2 McCabe-Thiele Diagram for Thorium.

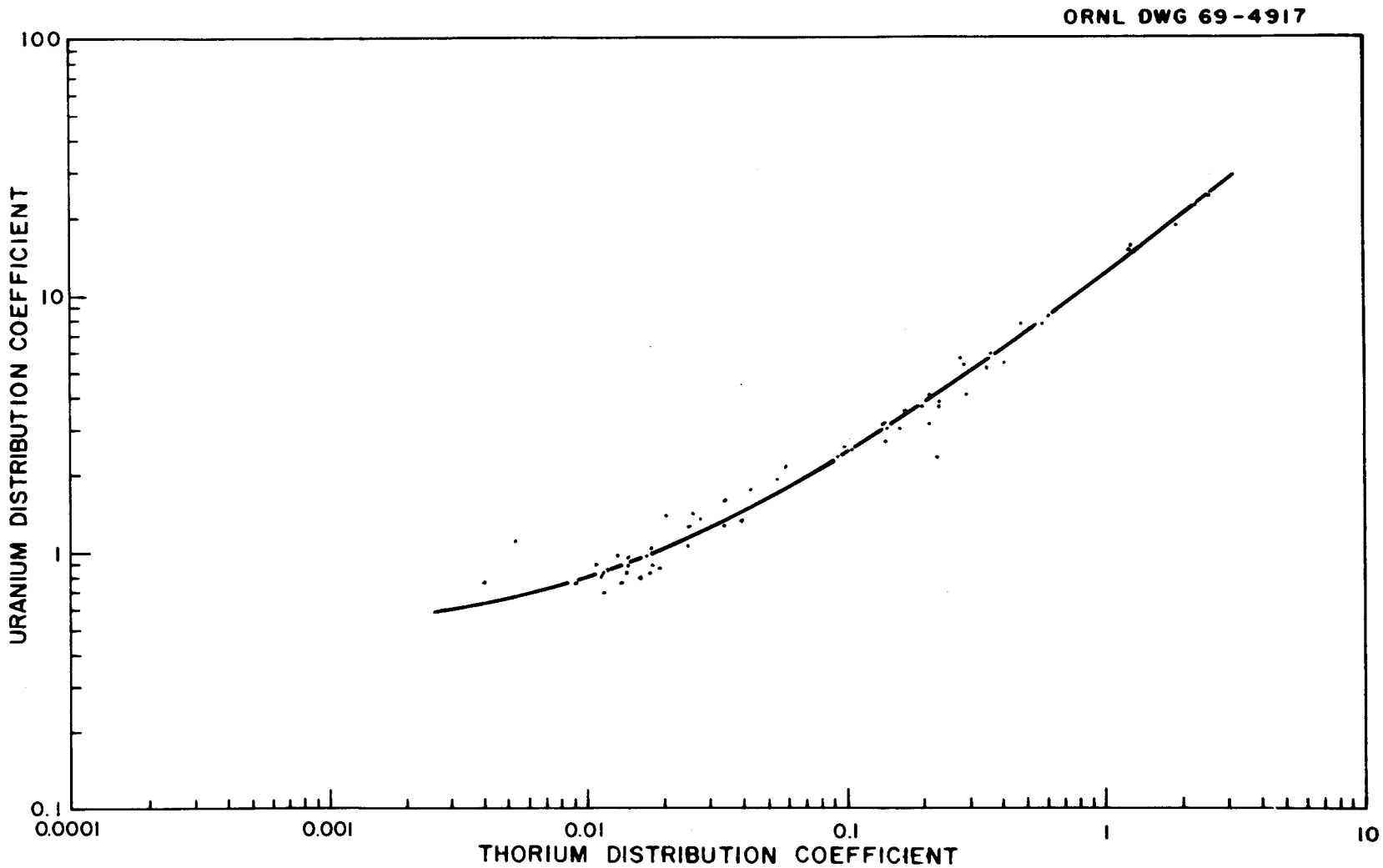

Fig. 1.3 Observed Relationship of Distribution Coefficients for Thorium and Uranium.

The results of the runs made during this quarter may be summarized as follows: Flow capacities averaged 1.61 liters/min and 1.00 liters/min in the extraction zone for aqueous-continuous and organic-continuous operation, respectively. These flow capacities correspond to maximum uranium processing rates of 49 and 30 kg/day. Uranium extraction in the aqueous-continuous mode was greater than 99.2% complete with 5 or more stages, and greater than 99.9% with 13 stages. In the organic-continuous mode, extractions were only about 97% complete in 5 stages, but were 99.5% and greater than 99.9% complete in 8 and 11 stages, respectively. Extraction stage efficiencies were low as compared with those normally experienced during the stacked-clone development program (i.e. using dilute chemical systems), but were comparable to those experienced with the Purex and Interim-23 type of flowsheets.[1,2] Scrubbing efficiencies were essentially nil for aqueous-continuous operation, but were similar to extraction efficiencies in the organic-continuous mode. This effect has been previously reported.[2] Satisfactory thorium-uranium decontamination factors were obtained for those runs in which considerable scrubbing was obtained.

The unique capabilities of the stacked-clone contactor have been pointed out on many occasions. However, the contactor does have limitations. Chief among these are its working range of flow ratios and its sensitivity to the physical properties of the chemical system. For example, the viscosity of the continuous phase is especially critical. The contactor operates effectively over a wide range of flow ratios and exhibits remarkably high flow capacities at very high ratios of continuous phase to dispersed phase; however, at ratios much below unity, the backmixing that occurs between stages is probably fairly extensive.

---

[1] M. E. Whatley *et al.*, Unit Operations Section Quarterly Progress Report, October-December 1966, ORNL-4094.

[2] M. E. Whatley *et al.*, Unit Operations Section Quarterly Progress Report, January-March 1967, ORNL-4139.

This tends to decrease the mass-transfer efficiency. Backmixing, which had produced low efficiencies in previous work with the Purex and Interim-23 types of systems, not only limited the aqueous-phase-continuous extraction efficiencies but also prevented scrubbing in this mode in the tests using simulated FBR reprocessing conditions.

In previous work, extraction stage efficiencies of at least 60% were usually achieved in the aqueous-continuous mode, while efficiencies of only 30 to 40% were noted in the organic-continuous mode.[3] In the most recent tests, the efficiencies obtained, namely, 35 to 60% in the aqueous-continuous mode and 35 to 45% in the organic-continuous mode, are in fairly good agreement with the earlier results. Scrubbing efficiencies in the organic-continuous mode were approximately equal to the extraction efficiencies.

Since backmixing effectively lengthens the solvent exposure time as well as restricts mass transfer, flowsheet parameters (especially flow ratios) should be adjusted, wherever possible, in order to exploit the advantages of the stacked-clone contactor to the fullest extent. Also, verification of organic-phase-continuous mass-transfer efficiencies with another system is recommended.

---

[3] M. E. Whatley *et al.*, *Unit Operations Section Quarterly Progress Report, October-December 1967*, ORNL-4235 (in press).

2. MOLTEN-SALT REACTOR PROCESSING STUDIES

L. E. McNeese

A molten-salt breeder reactor (MSBR) will be fueled with a molten fluoride mixture that will circulate continuously through the reactor core and the primary heat exchanger. A close-coupled processing facility for removing fission products and fissile materials from this mixture will be an integral part of the reactor system.

Low-pressure distillation is one method being considered for separating the rare-earth fission products (i.e. fission products having fluorides of low volatility) from the more-volatile components of the fuel salt. Experimentally determined relative volatilities indicate that adequate removal of the rare-earth fluorides from fuel salt can be accomplished. Results of distillation experiments with nonradioactive salt having the composition of the MSRE fuel carrier salt, $LiF-BeF_2-ZrF_4$ (65-30-5 mole %), are presented.

In order to obtain a high breeding ratio in an MSBR, a low protactinium concentration must be maintained in regions of high neutron flux. This avoids parasitic capture in the protactinium before it decays to uranium. Presently, the main emphasis is on processing a single-fluid MSBR in which protactinium must be separated from uranium, thorium, and fission products.

A flowsheet that uses reductive extraction for isolating protactinium from a single-fluid MSBR has been proposed, and results of the performance of the isolation system under steady-state conditions have been calculated. These calculations were based on laboratory data on the distribution of materials of interest between molten salt and liquid bismuth containing a reductant.

2.1 MSRE Distillation Experiment

J. R. Hightower L. E. McNeese

Distillation is one of the processes being considered for removing rare-earth fission products from MSBR fuel salt. Equipment has been built for demonstrating this process step. The system, which has been described previously,[3,4] will be used to distill a 48-liter batch of fuel salt from the MSRE; it is now undergoing nonradioactive testing before being installed at the MSRE. Two 48-liter batches of simulated MSRE fuel carrier salt, $LiF-BeF_2-ZrF_4$ (65-30-5 mole %) have been distilled.

2.1.1 Operating Procedures

To start a run, the still pot was heated to 900°C, and the entire system was evacuated to about 5 mm Hg. The valve between the feed tank and the vacuum pump was then closed (see Fig. 2.1), and argon was fed into the feed tank in order to force salt into the still. The condenser pressure was then reduced to 0.5-0.05 mm Hg, where the vaporization rate became appreciable. At this time, the system was put on automatic control. Salt was fed to the still pot at a rate necessary to maintain a nearly constant liquid level in the still. A level sensor opened the argon feed valve to the feed tank when the level decreased below a given point and closed the valve when the salt level in the still rose above another predetermined point.

The salt vapor condensed, then drained through a sample cup at the end of the condenser, and finally flowed into the condensate receiver. Samples of the condensate were withdrawn periodically by using a windlass to lower a small copper ladle (on the end of a cable) into the sample

---

[4] M. W. Rosenthal, MSR Program Semiann. Progr. Rept. Feb. 28, 1967, ORNL-4119, p. 211.

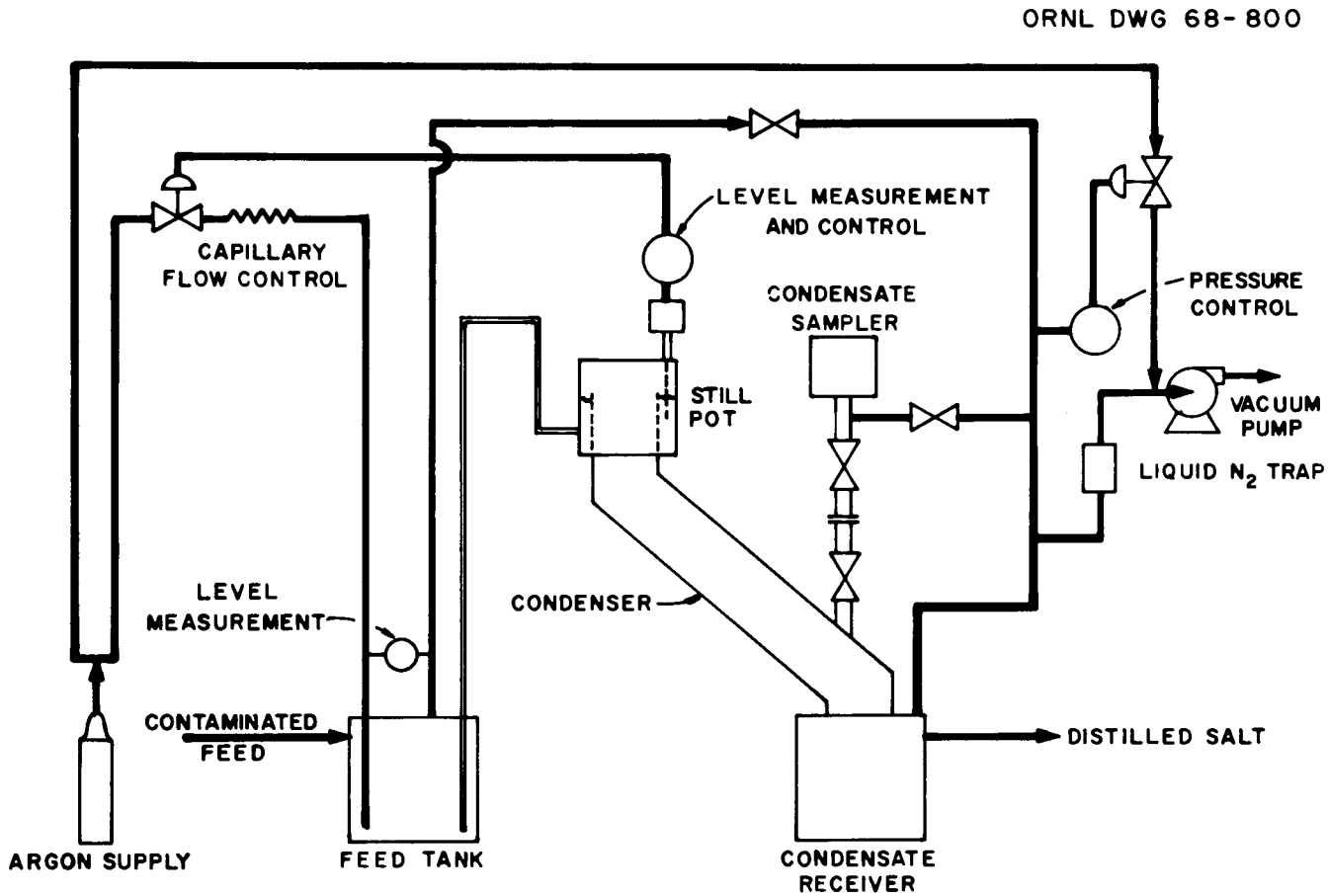

Fig. 2.1 Flow Diagram for Molten Salt Distillation Experiment.

cup. The sealed assembly containing the windlass, cable, and sample ladle could be connected to, and removed from, the still without disturbing the run. Each sample consisted of 8 to 10 g of condensate.

At the end of the run, the remaining salt in the feed tank was used to flush the high-melting salt from the still pot to produce salt having a liquidus temperature of less than 700°C. A total of about two liters of salt was transferred to the receiver by overflowing the still pot. The salt remaining in the still pot was then drained back into the feed tank.

2.1.2 Experimental Results

Two 48-liter batches of nonradioactive $LiF-BeF_2-ZrF_4$ (65-30-5 mole %) were distilled in the molten-salt still. Distillation rates were measured during the runs under various operating conditions by measuring the rate of change of the salt level in the feed tank and in the condensate receiver while the volume of salt in the still pot was held constant. These rates, along with the conditions under which they were measured, are summarized in Table 2.1.

The distillation was found to be, roughly, a linear function of condenser pressure (for the pressures considered) at constant still temperature, but appeared to be a somewhat stronger function of still temperature at approximately constant condenser pressure. The data indicate that the distillation rate in the molten-salt still is determined by the pressure drop between the vaporization surface and the condensation surface. With a condenser pressure of about 0.06 mm Hg, the distillation rate increased approximately 20% as the temperature of the still pot was increased from 990 to 1005°C. This change in temperature corresponds to a 20% increase in salt vapor pressure and correlates favorably with the observed increase in distillation rate.

Four condensate samples were taken during the first run; two were taken during the second run. The analyses from the first run (MSS-C-1) are summarized in Table 2.2. Results from the second run are not yet available.

Table 2.1. Distillation Rates Measured in the Molten-Salt Still

Still Pot Temperature (°C)	Condenser Pressure (mm Hg)	Duration of Test (hr)	Vaporization Rate (ft^3 salt/day · ft^2)[a]
990	0.5	7.2	1.15
990	0.3	9.5	1.20
990	0.055	16.5	1.25
1005	0.07	29.8	1.50

[a]Assuming a salt density of 2.2 g/cm^3.

Table 2.2 Analyses of Condensate Samples from Molten-Salt Still Run MSS-C-1

Volume Distilled (liters)	Component		
	BeF_2[a]	LiF[a]	ZrF_4[a]
0	0.554	0.248	0.199
13.0	0.335	0.622	0.0435
17.4	0.2900	0.665	0.0442
30.1	0.284	0.674	0.425

[a]Values are given in mole fractions.

If vapor having a composition equal to that of the first condensate samples is assumed to be in equilibrium with salt having the initial still pot composition (65-30-5 mole % LiF-BeF_2-ZrF_4), the relative volatilities for BeF_2 and ZrF_4, with respect to LiF, are 4.84 and 10.4, respectively. The relative volatility for BeF_2 compares favorably with the value of 4.7, which was determined in small recirculating equilibrium stills with liquid of the composition 85-10-5 mole % LiF-BeF_2-LnF_3. The relative volatility for ZrF_4, as determined in these tests, is higher than the range 0.76-1.4, which was determined previously for ZrF_4 concentrations of 0.03 to 0.98 mole %.[5]

2.1.3 Operational Difficulties

Although the operation of the still was, in general, surprisingly smooth, some difficulties were encountered. These difficulties involved the conductivity-type liquid-level indicators in the still pot, the condensate sampling arrangement, and a deposit that developed in the feed line to the still.

[5]J. R. Hightower and L. E. McNeese, Measurement of the Relative Volatilities of Fluorides of Ce, La, Pr, Nd, Sm, Eu, Ba, Sr, Y, and Zr in Mixtures of LiF and BeF_2, ORNL-TM-2058 (January 1968).

2.1.3.1 Conductivity-Type Level Indicators. — The level indicators in the still pot essentially measure the total conductance between a metal probe (extending into the molten salt) and the wall of the still pot. The total conductance is a function of the immersed surface area of the probe.[6] At the beginning of the first run, when salt was transferred from the feed tank at 550°C and about 4.5 psia to the still pot at 900°C and an absolute pressure of 5 mm Hg, the signal from the level indicators became extremely noisy. Because of the noise, the salt level in the still had to be maintained between two points where the signal was known to be discontinuous. The discontinuities allowed manual control of the level between the two known points even though the signal was noisy; however, the volume of salt in the still pot was about 9.4 liters instead of 12.3 liters, the design volume. The noise was probably caused by the evolution of dissolved argon and the simultaneous formation of bubbles on the surface of the level probes as the salt was heated under low pressure. After the salt had been at still pot conditions for about 4 hr, the noise abated and automatic operation was started. No similar noise occurred at the beginning of the second run. The feed salt for that run had been in the feed tank for only a few hours prior to the run, as compared with a month in the case of the first run.

Other undesirable effects shown by the level indicators were the temperature dependence of the output signal and the decrease in sensitivity when the level was near the overflow point in the still pot. The temperature dependence prevented our obtaining a good calibration curve that would be valid for the operating conditions of the still.

2.1.3.2 Sampling Difficulties. — During the second run, vapor condensed and solidified in the line through which the condensate samples were withdrawn. This blockage prevented the ladle from reaching the sample cup. During the run, the line was heated for short periods to 600°C in

---

[6] M. W. Rosenthal, MSR Program Semiann. Progr. Rept. Feb. 28, 1967, ORNL-4119, p. 76.

an attempt to melt the solidified material; however, this effort was unsuccessful. After the run had been completed, the line was heated to about 800°C. Observation through a sight glass bolted on the sample flange showed that the condensate did not drain from the pipe walls. Instead, it sublimed, and the vapors had to be swept into the receiver by a rapid flow of argon.

2.1.3.3 Feed Line Deposit. — During the distillation of the second batch of salt, the salt feed line to the still pot became obstructed. The effects of the obstruction became noticeable after 24 hr of operation, although operation of the still was not interrupted. These effects consisted of an oscillating pressure in the feed tank (oscillations with a period of approximately 90 min) and two large deviations of the salt level (in the still pot) from the set point.

During the period when the still pot was being flushed, the feed line was heated to 950°C by salt flowing from the still pot to the feed tank. The deposit did not melt or dissolve.

When the obstructed section of the line (which was located by X-ray) was removed, the horizontal section just ahead of the still pot (see Fig. 2.1) was found to contain a porous, magnetic material. This material, some of which was gray and some of which was brass-colored, is being analyzed to determine the reason for its deposition.

2.1.4 Conclusions

The following conclusions can be drawn from the results of distilling the first two batches of MSRE fuel carrier salt:

1. Most of the instruments and equipment for the MSRE distillation experiment performed satisfactorily. Only minimal effort by an operator was required to maintain continuous operation of the still after the initial startup.

2. A more reliable level-measuring system will be required for determining the liquid level in the still pot in future distillation systems. A system (such as that used in the MSRE

drain tanks) that gives single-point level indications would be more desirable than the present system.

3. Vapor condensation in sample lines and vacuum lines is a potentially serious problem. An effective means of removing this condensate without affecting the operation of the still must be found.

4. The cause for the deposit in the feed line must be determined, and its significance as a recurring phenomenon must be assessed.

5. The distillation rate appears to be set by the pressure drop between the vaporization surface and the condensing surface.

6. When operated at the maximum flux observed in these experiments, an MSBR processing plant treating 15 ft^3 of fuel salt per day would require a still with a vaporization surface of about 10 ft^2.

2.2 Removal of Protactinium from a Single-Fluid MSBR

L. E. McNeese M. E. Whatley

Laboratory experiments have shown that protactinium and uranium can be extracted into bismuth from molten salt that contains the fluorides of lithium, beryllium, and thorium by using metallic thorium as the reductant. A flowsheet (Fig. 2.2) has been proposed for isolating protactinium from a single-fluid molten-salt breeder reactor, and results of the performance of the isolation system at steady state have been calculated, based on tentative values obtained from the laboratory experiments. In the proposed flowsheet, a salt stream from the reactor enters the bottom of the extraction column and flows countercurrently to a stream of bismuth containing reduced metals. Ideally, the metal stream entering the top of the column contains sufficient thorium and lithium to extract only the uranium entering the column. The system exploits the fact that protactinium is less noble than uranium but more noble than thorium. Hence, in the lower part of the column, uranium is

ORNL DWG 68-2082

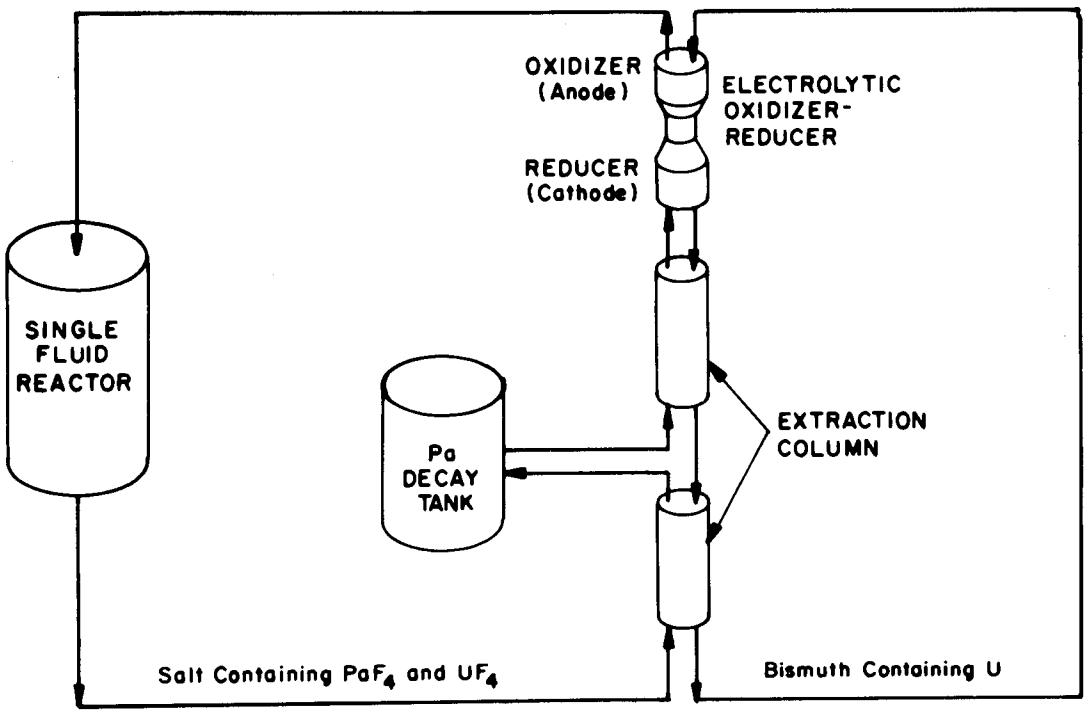

Fig. 2.2 Single-Fluid MSBR Processing by Reductive Extraction.

preferentially extracted from the incoming salt while the protactinium progresses farther up the column to the point where it is reduced by thorium. In this manner, protactinium refluxes in the center of the column, and relatively high protactinium concentrations result. A tank is provided at the center of the column, where the maximum protactinium concentration in the salt occurs, to retain the protactinium until it decays to uranium.

An essential part of the flowsheet is an electrolytic oxidizer-reducer, which has two purposes: (1) it recovers the extracted uranium from the metal stream leaving the extraction column, and (2) it prepares the lithium-thorium-bismuth stream that is fed to the extraction column. The metal phase containing the uranium extracted in the column serves as the cell anode, where uranium and lithium are oxidized to UF_4 and LiF. Salt from the top of the extraction column functions as the cell electrolyte; it first passes over a pool of liquid bismuth, which serves as the cathode, where thorium and lithium are reduced.

Calculated results showing typical performance of the protactinium isolation system are given in Fig. 2.3 for a case that we will consider to be the reference case. The minimum protactinium concentration in the reactor is obtained when the bismuth flow rate is just sufficient to extract the uranium that enters the system. At slightly higher bismuth flow rates, protactinium will also be extracted, since it is the next component in order of decreasing nobility. At bismuth flow rates slightly lower than the optimum rate, some uranium will not be extracted; this uranium and most of the protactinium will flow out the top of the column. In either case, some protactinium is allowed to return to the reactor, thereby diminishing the effectiveness of the system. The protactinium isolation system becomes ineffective almost immediately for bismuth flow rates lower than the optimum rate; for bismuth flow rates higher than the optimum rate, the protactinium concentration in the reactor increases from the minimum value (22 ppm) at the rate of 28 ppm per percent of increase in metal flow rate for the conditions of the reference case. Thus far, only the effects of variations in the bismuth flow rate on performance have been discussed; however, similar effects

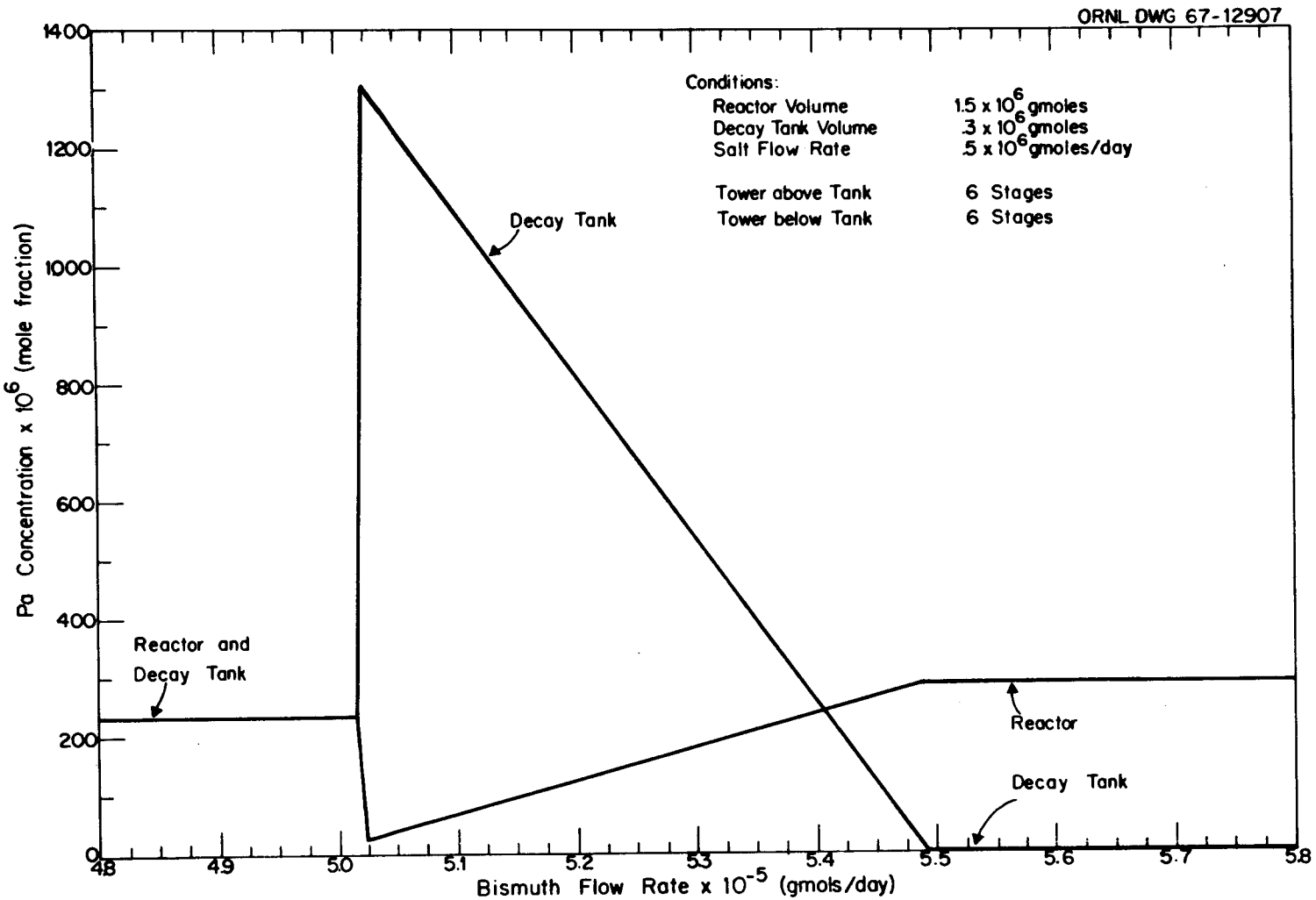

Fig. 2.3 Effect of Bismuth Flow Rate on Protactinium Concentration for Reference Case.

would be produced by variations in the salt flow rate or in the total concentration of reduced metals (equivalents of reduced metals per mole of bismuth) fed to the column. Calculated concentration profiles in the extraction column are shown in Fig. 2.4 for steady-state operation under optimum conditions. The concentration of uranium in the salt decreases from 3×10^{-3} mole fraction in the reactor to 6.3×10^{-5} mole fraction at the inlet to the protactinium decay tank, whereas the protactinium concentration increases from 2.2×10^{-5} mole fraction in the reactor to 1.32×10^{-3} mole fraction at the inlet to the decay tank. The concentrations of protactinium and uranium in the decay tank are 1.3×10^{-3} and 8.3×10^{-5} mole fractions, respectively. Above the decay tank, the uranium and protactinium concentrations decrease steadily to negligible values.

The flowsheet has several very desirable characteristics; these include a negligible holdup of fissile ^{233}U in the processing plant, an almost immediate return of newly produced ^{233}U to the reactor system, and a closed system that precludes loss of protactinium, ^{233}U, or other components of the reactor fuel salt. However, the protactinium removal efficiency is undesirably sensitive to minor variations in operating conditions (e.g. the salt or bismuth flow rate and the concentration of reduced metals in the bismuth stream that is fed to the extraction column). Methods for making the system performance less sensitive to such variations have been studied. The removal of uranium from the center of the column by fluorination of the molten salt was found to make the performance of the system at steady state insensitive to small changes in operating conditions; the concentration of UF_6 in the fluorinator off-gas was found to be extremely sensitive to changes in operating conditions and thus can be used as the primary process control point.

The effectiveness of a system stabilized by uranium removal has been compared with that of a nonstabilized system. In this comparison, we assumed that the error in the control of the bismuth flow rate was distributed normally around a best mean flow rate, FMB_o, with a standard

ORNL DWG 67-12893

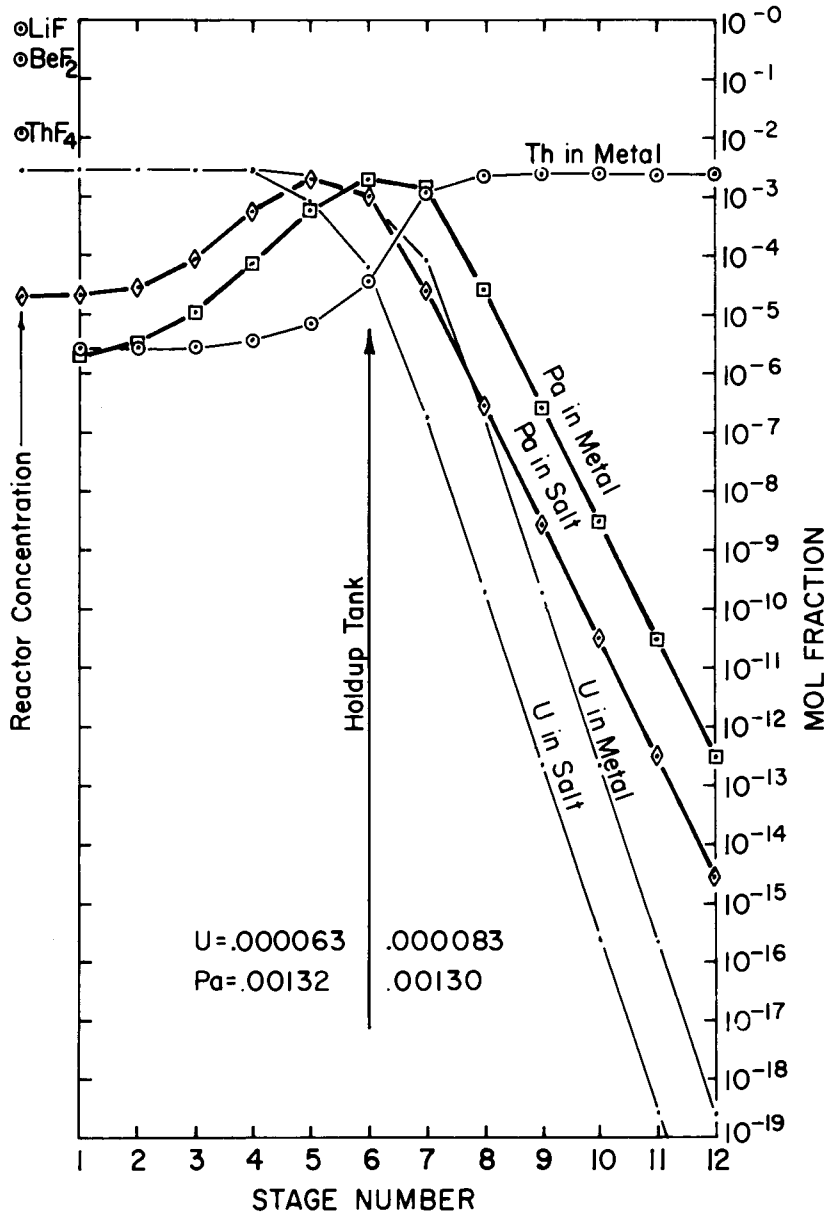

Fig. 2.4 Calculated Concentration Profiles in Reductive Extraction Tower for Reference Case at Optimum Bismuth Flow Rates.

deviation σ, so that the average protactinium concentration in the reactor, $\bar{c}$, could be calculated by:

$$\bar{c} = \frac{1}{\sqrt{2\pi}} \int_{-\infty}^{\infty} c(x) e^{-x^2/2} \, dx,$$

where

$$x = \frac{FMB - FMB_o}{\sigma},$$

FMB = bismuth flow rate,

c(x) = concentration of protactinium in the reactor at steady-state conditions at a bismuth flow rate corresponding to x.

Figure 2.5 shows the average protactinium concentration in the reactor as a function of the standard deviation of bismuth flow rate for cases with stabilization by uranium removal, as well as for two cases with no uranium removal. Protactinium processing cycle times of 1 day and 3 days (reference case) were used. For a standard deviation of 0.35% of FMB_{opt} (optimum bismuth flow rate), the minimum reactor protactinium concentration (22 ppm) is obtained if the fraction of uranium removed from the inlet to the decay tank is 2% or greater; with no uranium removal the average concentration is 38.5 ppm. With a protactinium processing cycle time of 1 day and a standard deviation of 0.35%, an average concentration of 24.5 ppm is obtained. For standard deviations larger than about 0.35%, a protactinium isolation system featuring a 1-day processing cycle time and no uranium removal produces approximately the same average protactinium concentration in the reactor as a system featuring a 3-day cycle time and removal of 1% of the uranium from the salt stream entering the decay tank.

In choosing the optimum protactinium isolation system, the relative costs associated with higher processing rates, closer process control, and increased uranium removal must be considered. These costs must then

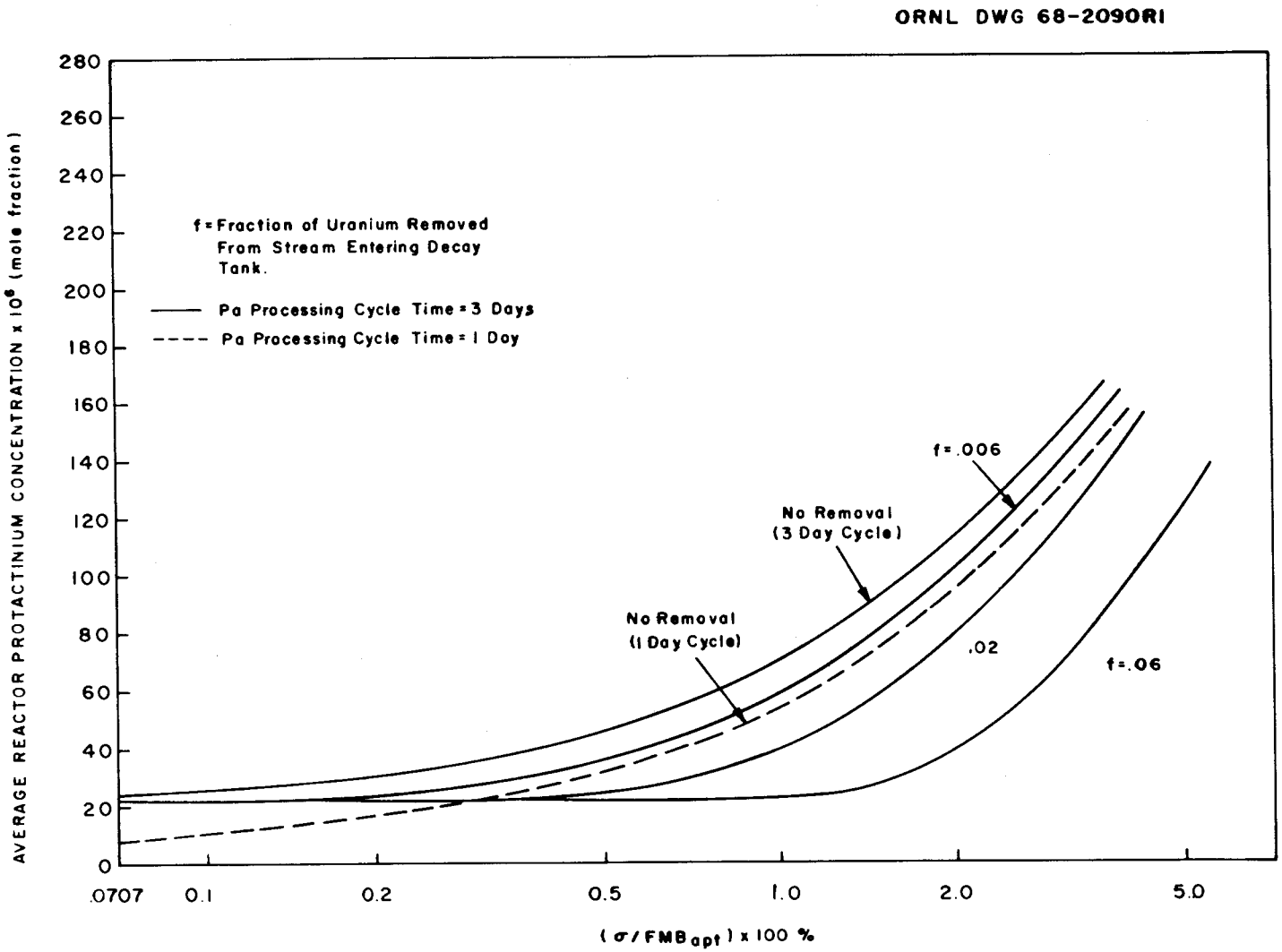

Fig. 2.5 Variation of Average Reactor Protactinium Concentration with Standard Deviation of Bismuth Flow Rate for Cases with Stabilization by Fluorination and with No Stabilization.

be weighed against the value of obtaining a given average protactinium concentration in the reactor. Further attention will be given to the transient operation of a protactinium removal system such as that described.

2.3 Continuous Fluorination of Molten Salt

B. A. Hannaford L. E. McNeese

Uranium in the fuel stream of an MSBR must be removed prior to the distillation step since UF_4 will not be completely volatilized during this operation. Equipment is being developed for the continuous removal of UF_4 from a salt stream by countercurrently contacting the salt with fluorine in a salt-phase-continuous system. The equipment will be protected from corrosion by freezing a layer of salt on the vessel wall; the heat necessary for maintaining molten salt adjacent to the frozen salt layer will be provided by the decay of fission products in the salt stream. Recent development work has been directed toward demonstrating the operability of a frozen-wall fluorinator using a countercurrent flow of molten salt and an inert gas.

The experimental equipment consisted of a 5-in.-diam by 8-ft-high column, fabricated from sched 40 nickel pipe (Fig. 2.6). An internal heat source consisting of three Calrod heaters contained in a 3/4-in.-diam sched 40 Inconel pipe was used to simulate a volume heat source in the molten salt. Two sets of internal thermocouples located near the center of each of two test sections indicated the radial temperature gradient, from which the location of the interface between molten and frozen salt could be inferred. Each test section was independently cooled by air flowing through spirally wound 3/8-in.-diam nickel tubing. Additional Calrod heaters were wound on the external surface of the fluorinator to provide auxiliary heat during heat-up and to provide control of the temperatures at the ends of the column. A 66-34 mole % $LiF-ZrF_4$ mixture, which has a liquidus temperature of 595°C and a phase

ORNL DWG 68-3340

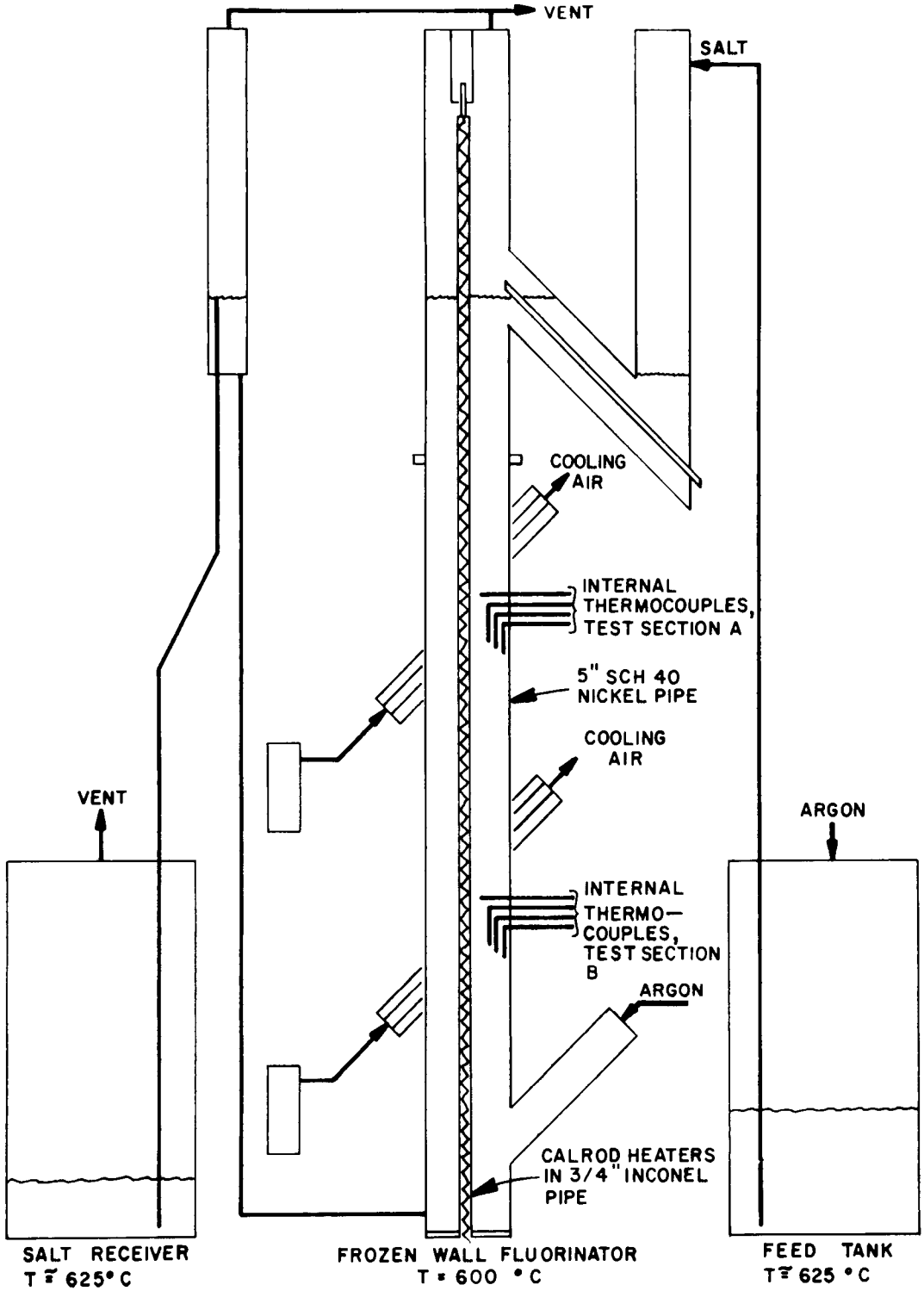

Fig. 2.6 Experimental Equipment for Studying the Formation of a Frozen Salt Layer for Corrosion Protection. Height of column = 8 ft. Height of each test section = 1.75 ft.

diagram similar to the $LiF-BeF_2$ system, was metered from the feed tank for periods as long as 5 hr. This allowed data to be collected for a 1- to 2-hr period of steady-state operation.

In these experiments we achieved our principal objective, namely, demonstration that a layer of frozen salt could be formed and maintained under approximate operating conditions. In Table 2.3, experimental conditions are compared with reference conditions for a fluorinator having a salt throughput of 15 ft^3/day, an inlet uranium concentration of 0.8 kg per ft^3 salt, and a 50% fluorine utilization.

Table 2.3 Comparison of Experimental and Reference Conditions for Fluorination of 15 ft^3 of Molten Salt per Day

	Experimental	Reference
Salt flow rate, liters/hr	~ 3.3	17.7
Gas flow rate, liters/min at STP	0.5-2.0[a]	2.0[b]
Heat flux, w/ft of column height	600-1600	~ 2000

[a]Argon.

[b]Fluorine.

In general, the thickness of the frozen wall and the temperature profiles in the frozen salt were in good agreement with the values predicted by relationships obtained by assuming only radial heat flow from a volume heat source. The thickness of the frozen wall ranged from 0.3 to 0.8 in. The effect of heat generation in the layer of frozen salt was not simulated in these experiments.

The thermal conductivity of the frozen salt was calculated, for each run, from the experimentally determined temperature gradient and the measured heat flux; the relative agreement of calculated values was considered to be indicative of the consistency of the experimental data. Thermal conductivities calculated from data for the upper test section

were closely grouped around 0.75 Btu/hr • ft •°F; however, values from the lower section were more widely scattered and were generally about 100% higher.

The heating-cooling system used on the column produced some variation in external wall temperature (and hence frozen wall thickness); in a typical run the difference between the liquidus temperature of the salt and the wall temperature ranged from 85 to 140°C.

In future experiments, the heat flux will be increased to the reference value, whereas the salt flow rate will be increased to approximately 50% of the reference rate.

2.4 Removal of Nickel, Iron, and Chromium Fluorides from Simulated MSRE Fuel Carrier Salt

L. E. McNeese J. H. Shaffer*

Current plans for the MSRE call for substituting ^{233}U for the mixture of ^{235}U and ^{238}U presently in the fuel salt. The fuel carrier salt, $LiF-BeF_2-ZrF_4$ (65-30-5 mole %), together with its fission product inventory, will be retained; this will be accomplished by, first, fluorinating the fuel salt to remove uranium and, then, adding ^{233}U in the form of a eutectic salt of the composition $LiF-UF_4$ (73-27 mole %).

During fluorination, the salt will become contaminated with the fluorides of nickel, iron, and chromium as a result of the corrosion of the fluorinator, which is constructed of Hastelloy N. Although, under normal conditions, these fluorides are expected to be dissolved in the fuel salt, their return to the reactor is undesirable for several reasons. First, chromium in high concentrations will decrease the sensitivity of chromium analyses and, hence, will decrease the accuracy of assessing generalized corrosion during operation. Second, fluorides of nickel and iron will react with chromium, which is the least noble constituent of Hastelloy N. We have performed experiments which indicate that the Ni(II) can be reduced by hydrogen sparging and that the Fe(II)

*Reactor Chemistry Division.

and the Cr(II) can be reduced by the addition of zirconium metal. Filtration of the resulting mixture of salt and reduced metals was shown to be effective for removing suspended metals.

2.4.1 Reduction of Corrosion-Product Fluorides

The experimental program was carried out with a 104-kg batch of the fluoride mixture, $LiF-BeF_2-ZrF_4$ (65-30-5 mole %), which was prepared from the component fluoride salts by routine production procedures. Initial treatment of the molten mixture with $HF-H_2$ (1:10 volume ratio) removed oxygen and sulfur impurities. In order to represent conditions that are expected after fluorination of the MSRE fuel salt, approximately 80 of CrF_2, 50 g of FeF_2, and 800 g of NiF_2 were added to the salt mixture, which was then hydrofluorinated for 6 hr with 10 to 20 mole % HF in helium to ensure complete dissolution of the corrosion-product fluorides. The results obtained from chemical analysis of a filtered salt sample taken after hydrofluorination are compared with estimated concentrations in Table 2.4.

Table 2.4 Concentrations of Corrosion-Product Fluorides After Hydrofluorination

Material	Quantity (g)	Estimated Concentration (ppm)[a]	Results from Chemical Analysis (ppm)[a]
CrF_2	80	445	470
FeF_2	50	286	620
NiF_2	800	4680	3700

[a]Concentrations reported on a metal basis.

Calculations showed that reduction of the quantity of corrosion-product difluorides anticipated from the prepared salt mixture would require approximately 11.4 equivalents of reductant per cubic foot of salt mixture. Equilibrium data[7] for the reduction (see Table 2.5) indicate that, if equilibrium is achieved, hydrogen sparging will reduce Ni(II) easily, Fe(II) with difficulty, and Cr(II) to a negligible extent in a practical time period. The aim of the first part of the experiment was to demonstrate the reduction of Ni(II) with a hydrogen sparge and to compare hydrogen utilization with that predicted from equilibrium data. After the initial hydrofluorination, free HF was stripped from the salt mixture by helium sparging, and the molten salt was sparged for 9 hr with hydrogen at the rate of 10 liters/min (STP) at 650°C. The 48.2-liter salt mixture was contained in a 12-in.-diam vessel; the sparge line terminated 26 in. below the melt surface. The gas effluent from the treatment vessel was analyzed periodically for HF (Fig. 2.7), and sparging was discontinued when the HF concentration decreased to a low, but nearly constant, value. The quantity of HF produced during this period was equivalent to about 93% of the NiF_2 initially present in the salt mixture. Hydrogen utilization was considerably lower than would have been the case if equilibrium had been achieved; under equilibrium conditions a sparge time of 20.4 min would have resulted in reduction of 99% of the Ni(II) initially present.

Table 2.5 Equilibrium Quotients for the Reduction of Corrosion-Product Fluorides in $LiF-BeF_2$ (62-38 mole %) at 650°C

Metal Fluoride	K_Q (atm) $= \frac{P^2_{HF}}{(P_{H_2})\ N_{MF_2}}$
NiF_2	2.9×10^4
FeF_2	2.8×10^{-1}
CrF_2	$\sim 1 \times 10^{-5}$

[7] C. M. Blood, Solubility and Stability of Structural Metal Difluorides in Molten Fluoride Mixtures, ORNL-CF-61-5-4 (Sept. 21, 1961); also issued as ORNL-TM-760.

ORNL DWG 68-4134RI

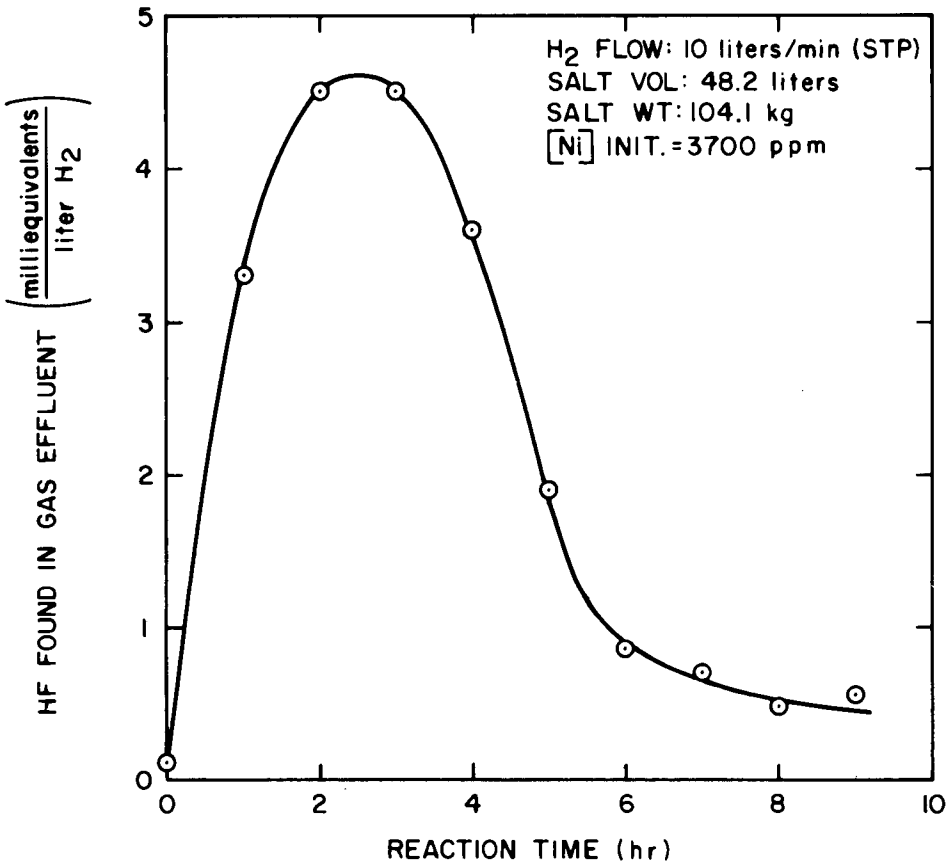

Fig. 2.7 Evolution of Hydrogen Fluoride During the Reduction of Corrosion-Product Fluorides with Hydrogen.

Since equilibrium data predict a very low hydrogen utilization during the reduction of Fe(II) and Cr(II), data concerning the reduction of these metal ions with zirconium metal were obtained. The zirconium was machined first in order to increase the surface area and, thereby, to reduce passivation of the surface by deposition of reduced iron and chromium. To facilitate their addition to the treatment vessel, the turnings were pressed into 3/4-in.-diam cylinders ($\rho = \sim 4.6$ g/cm^3) having lengths of 0.3 to 1.0 in. The pressed zirconium cylinders were added to the salt mixture after the Ni(II) had been reduced by means of hydrogen sparging. After each addition, the approximate extent of reduction was noted by sparging the melt with hydrogen and analyzing the effluent gas for HF. The HF concentration decreased steadily (Fig. 2.8), and an arbitrary end point for the reduction reaction was established at a concentration of 0.02 meq of HF per liter of hydrogen. This concentration was chosen as a result of previous experience during the preparation of the initial MSRE fuel carrier salt. The calculated quantity of zirconium required to complete the reduction of the corrosion-product fluorides was 115 g; this quantity was based on the analysis of the salt mixture (shown in Table 2.4) and assumed the reduction of 12.2 equivalents of these metal fluorides during the hydrogen reduction period. Analyses of filtered samples taken near the conclusion of the zirconium addition period are shown below.

Quantity of Zirconium Added (g)	Quantities of Metals Found (ppm by wt)		
	Cr	Fe	Ni
253	9	60	< 30
327	26	44	36

These values are below the limits established for the initial MSRE fuel carrier salt. On the basis of these data, zirconium utilization was at least 46 to 65%.

ORNL DWG 68-4135R1

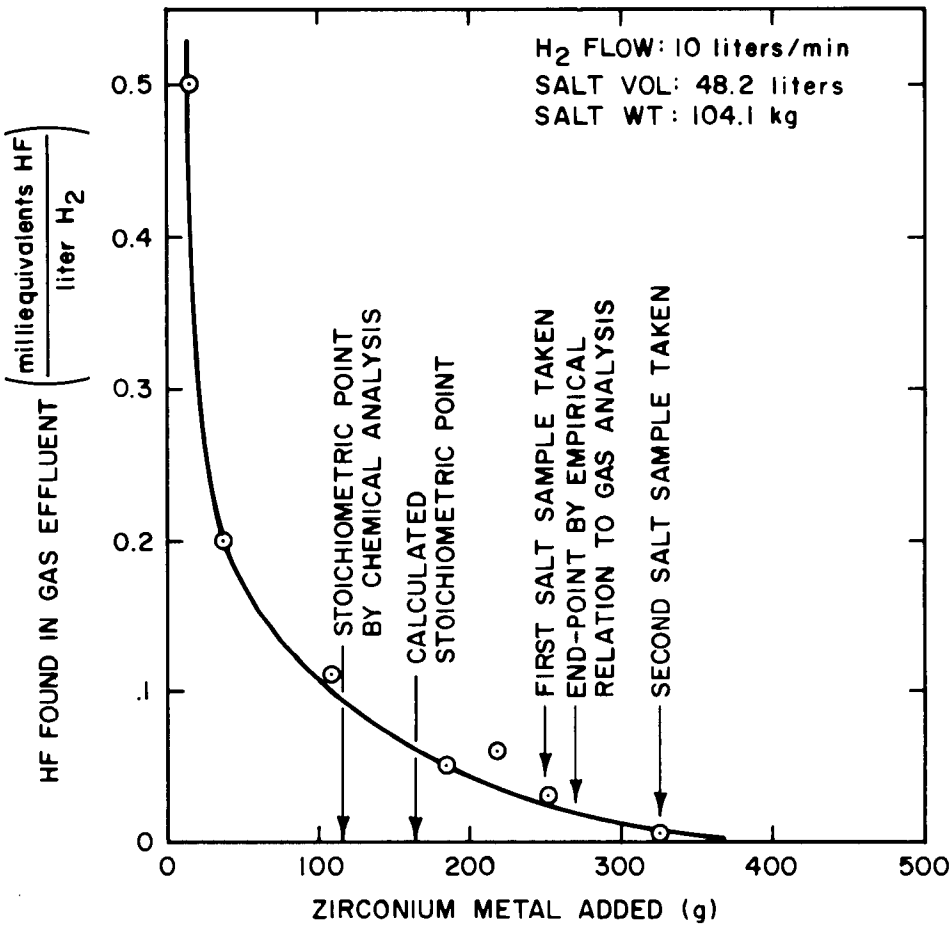

Fig. 2.8 Evolution of Hydrogen Fluoride During the Reduction of Corrosion-Product Fluorides with Zirconium.

2.4.2 Salt Filtration Studies

The reduction of corrosion-product fluorides from the MSRE fuel-carrier salt may produce as much as 330 g of metals per cubic foot of salt mixture. Since suspension or entrainment of a major fraction of these solids during the transfer of the fuel salt to the reactor drain tank could adversely affect filter performance, tests were made to determine salt-filtration characteristics under conditions which approximate those that are anticipated in the reactor application.

Filtration tests were conducted using three filters: a sintered nickel filter* having a mean pore diameter of 40 μ, and two grades of Feltmetal.** Each filter was fabricated as a 2-5/8-in.-diam plate in order that the geometric surface areas of all filters would be identical. The first grade of Feltmetal consisted of Monel having a mean pore diameter of 20 μ, while the second consisted of 347 stainless steel having a mean pore diameter of 41 μ. The latter material (designated FM250 by the manufacturer) had a porosity of 78% and a stated removal efficiency of 98% for particles larger than 10 μ in diameter. This material was chosen for application in the reactor system because of its adaptability to fabrication requirements and its satisfactory performance during the filtration tests .

In establishing the credibility of the multiple filtration tests that were performed using the same batch of salt, we have assumed that the primary solids-removal process is decantation. This assumption was based on considerable experience in filtering fluoride mixtures through sintered nickel. Examination of filters used in this manner has consistently shown the retention of very small quantities of solids, although considerable quantities of solids accumulate in the salt treatment vessels during repeated use in the production process.

---

*Micro Metallic Div. of Pall Corp., Glen Cove, L. I., N. Y.

**Huyck Co., Rensselaer, N. Y.

The experimental assembly used for the filtration tests was essentially that used for the routine production of fluoride mixtures. The salt-preparation vessel was connected by a 1/2-in.-diam Inconel tube to a heated salt-receiver vessel. The transfer tube extended to within 1/4 to 1/2 in. of the bottom of the salt-preparation vessel and only penetrated the top of the receiver. The filter was mounted vertically in the transfer line above the receiver vessel. A salt return line extended from near the bottom of the receiver vessel to the salt-preparation vessel. This arrangement permitted eight filtration tests to be made with the same batch of salt.

Although conditions that would promote decantation are desired for the reactor application, attempts were made also to observe filter-loading capacities. Some tests were made under static conditions by allowing the melt to remain quiescent for a minimum of 4 hr prior to transfer; some were also made by rapidly sparging the melt with helium just prior to salt transfer. The temperature of the melt was controlled at 650°C in each case. The temperature of the salt-transfer line was maintained at about 565°C during the transfer operations. The salt was transferred by pressurizing the treatment vessel with helium to 11 psig and evacuating the receiver vessel. These conditions were maintained throughout each test, so that the pressure drop across the filter varied from 22.5 to 20.8 psi as the level of salt in the treatment vessel decreased.

A summary of the filtration tests is shown in Table 2.6. The 20-μ Feltmetal was tested first, and was rejected after 2 hr of operation; essentially no salt passed through the filter during this period. Inspection of the filter showed that the major part of the 22-g holdup was salt; only a thin layer of metallic material was observed on the filter plate. The second test was made with sintered nickel; the entire 1.7 ft^3 of salt was filtered in 0.5 hr, and 7 g of material was collected on the filter plate. Since no visible failure of the filter plate was apparent, we presume that either the decantation process was extremely efficient or the suspended particles were too small to be removed by the filter. The remaining filtration tests showed comparable results that

Table 2.6 **Summary of Filtration Tests**

Salt composition: $LiF-BeF_2-ZrF_4$ (65-30-5 mole %)
Weight of salt mixture: 104.1 kg
Volume of salt at 650°C: 1.7 ft^3
Indicated pressure differential: 11 psig (forepressure vs vacuum)

Test No.	Filter Material	Pore Diameter (μ)	Salt Conditions	Transfer Time (hr)	Weight Gain (g)	Remarks
1	Monel Feltmetal	20	Static		22	Test terminated after 2 hr; essentially no salt transfer.
2	Sintered nickel	40	Static	0.5	7	No visible material on filter or evidence of failure.
3	Sintered nickel	40	Agitated	1.75	44	
4	347 SS Feltmetal	41	Static	2.0	77	Test stopped after transfer of 90 kg.
5	Sintered nickel	40	Static	2.17	63	Filter plugged after transfer of 40 kg. Material on filter predominantly salt.
6	Sintered nickel	40	Static	1.84	19	Balance of salt transferred; filter ruptured.
7	347 SS Feltmetal	41	Agitated	2.0	67	
8	Sintered nickel	40	Static	1.75	22	Back transfer of 80 kg salt from receiver to treatment vessel; filter plugged.

were essentially independent of the degree of agitation of the melt. Filtration times for FM250 Feltmetal were about 1.19 and 1.36 hr per cubic foot of salt mixture. (The longer transfer time probably reflected a lower salt temperature at the filter.) The occasional plugging of the filter in tests 4 and 5 suggests that the loading capacity of the 40-μ filters may be about 50 to 75 g of metal particles, or about 9 to 14 g per square inch of filter surface.

Samples of the salt mixture were withdrawn by means of a filter stick prior to the first filtration experiment and by a composite sampler located downstream from the filter plate after tests 4, 6, and 7. Analyses of these samples are given in Table 2.7. Although the filter ruptured in test 6, chemical analyses did not show excessive concentrations of metals in the filtered salt. Variations in the other results are probably within the combined reproducibility of the analytical methods and the test procedure. Only 1.8 to 3.4% of metals reduced from solution passed through the filter material that is proposed for use in the reactor application.

Table 2.7 Summary of Analytical Results During Filtration Tests

Filtered Sample	Impurity concentration (ppm)			
	Cr	Ni	Fe	Total
Before Test 1	26	36	44	106
After Test 4	15	84	66	165
After Test 6	16	256	132	404
After Test 7	17	19	49	85

ORNL-4364
UC-4 — Chemistry

INTERNAL DISTRIBUTION

1. Biology Library
2-4. Central Research Library
5-6. ORNL — Y-12 Technical Library
Document Reference Section
7-40. Laboratory Records Department
41. Laboratory Records, ORNL R.C.
42. R. E. Blanco
43. J. O. Blomeke
44. R. E. Brooksbank
45. K. B. Brown
46. F. R. Bruce
47. W. D. Burch
48. W. H. Carr
49. G. I. Cathers
50. J. M. Chandler
51. W. E. Clark
52. K. E. Cowser
53. D. J. Crouse
54. F. L. Culler, Jr.
55. W. Davis, Jr.
56. D. E. Ferguson
57. L. M. Ferris
58. J. R. Flanary
59. H. E. Goeller
60. J. M. Googin (Y-12)
61. H. B. Graham
62. A. T. Gresky
63. P. A. Haas
64. F. E. Harrington
65. R. F. Hibbs
66. R. W. Horton
67. G. Jasny (Y-12)
68. H. F. Johnson
69. W. H. Jordan
70. S. H. Jury
71. L. J. King
72. B. B. Klima
73. E. Lamb
74. D. M. Lang
75. R. E. Leuze
76. R. B. Lindauer
77. H. G. MacPherson
78. G. M. Marrow (Y-12)
79. J. L. Matherne
80. J. P. McBride
81. W. T. McDuffee
82. W. H. McVey
83. J. P. Nichols
84. E. L. Nicholson
85. F. L. Parker
86. J. R. Parrott
87. J. H. Pashley (K-25)
88. F. S. Patton, Jr. (Y-12)
89. R. H. Rainey
90. A. D. Ryon
91. W. D. Schaffer, Jr.
92. M. J. Skinner
93. Martha Stewart
94. J. C. Suddath
95. D. A. Sundberg
96. W. E. Unger
97-117. Unit Operations Section
118. C. D. Watson
119. A. M. Weinberg
120. M. E. Whatley
121. R. H. Winget
122. R. G. Wymer
123. E. L. Youngblood
124. P. H. Emmett (consultant)
125. J. J. Katz (consultant)
126. J. L. Margrave (consultant)
127. E. A. Mason (consultant)
128. R. B. Richards (consultant)

EXTERNAL DISTRIBUTION

129. E. L. Anderson, Atomic Energy Commission, Washington
130. A. L. Babb, University of Washington
131. F. P. Baranowski, Atomic Energy Commission, Washington
132. W. G. Belter, Atomic Energy Commission, Washington
133. S. Bernstein, Union Carbide Corporation, Paducah
134. D. E. Bloomfield, Battelle Northwest, Richland, Washington

135. J. A. Buckham, Idaho Chemical Processing Plant
136. J. T. Christy, Richland Operations Office
137. C. R. Cooley, Pacific Northwest, Richland, Washington
138. C. B. Deering, Atomic Energy Commission, Oak Ridge
139. E. R. Gilliland, Massachusetts Institute of Technology
140. W. W. Grigorieff, Assistant to the Executive Director, Oak Ridge Associated Universities
141. M. J. Harmon, Pacific Northwest, Richland, Washington
142. L. P. Hatch, Brookhaven National Laboratory
143. O. F. Hill, Pacific Northwest, Richland, Washington
144. C. H. Ice, Savannah River Laboratory
145. E. R. Irish, Pacific Northwest, Richland, Washington
146. B. M. Legler, Idaho Chemical Processing Plant
147. J. A. Lieberman, Atomic Energy Commission, Washington
148. B. Manowitz, Brookhaven National Laboratory
149. J. A. McBride, DML, Atomic Energy Commission, Washington
150. J. W. Nehls, Atomic Energy Commission, Oak Ridge
151. C. M. Nicholls, AERE, Harwell, England
152. E. O. Nurmi, Babcock and Wilcox Company
153. H. Pearlman, Atomics International
154. A. M. Platt, Pacific Northwest, Richland, Washington
155. R. A. Proebstle, Knolls Atomic Power Laboratory
156. J. W. Pollock, Idaho Operations Office
157. K. L. Rohde, Idaho Chemical Processing Plant
158. C. A. Rohrmann, Pacific Northwest, Richland, Washington
159. C. M. Slansky, Idaho Chemical Processing Plant
160. M. Smutz, Ames Laboratory, Ames, Iowa
161. C. E. Stevenson, Argonne National Laboratory, Idaho Falls
162. K. G. Steyer, General Atomic
163. J. A. Swartout, Union Carbide Corporation, New York
164. C. D. Tabor, Goodyear Atomic
165. V. R. Thayer, Du Pont Company, Wilmington
166. R. C. Vogel, Argonne National Laboratory
167. E. E. Voiland, Pacific Northwest, Richland, Washington
168. G. H. Wagner, General Electric Company, Santa Clara, California
169. Laboratory and University Division, AEC, ORO

170-374. Given distribution as shown in TID-4500 under Chemistry category (25 copies — CFSTI)